

Triaxial MEMS accelerometer with screen printed PZT thick film

Christian C. Hindrichsen · Ninia S. Almind ·
Simon H. Brodersen · Rasmus Lou-Møller ·
Karsten Hansen · Erik V. Thomsen

Received: 12 November 2008 / Accepted: 2 February 2010 / Published online: 13 February 2010
© Springer Science+Business Media, LLC 2010

Abstract Piezoelectric thick films have increasing interest due to the potential high sensitivity and actuation force for MEMS sensors and actuators. The screen printing technique is a promising deposition technique for realizing piezoelectric thick films in the thickness range from 10–100 μm . In this work integration of a screen printed piezoelectric PZT thick film with silicon MEMS technology is shown. A high bandwidth triaxial accelerometer has been designed, fabricated and characterized. The voltage sensitivity is 0.31 mV/g in the vertical direction, 0.062 mV/g in the horizontal direction and the first mode resonance frequency is 11 kHz. A Finite Element Method (FEM) model is used to validate the measured sensitivity and resonance frequency. Good agreement between the model and the measurements is seen.

Keywords Screen printing · PZT thick film · Piezoelectric effect · MEMS device · Triaxial accelerometer · Fabrication process flow · Characterization

1 Introduction

Many different Microelectromechanical systems (MEMS) utilize the piezoelectric effect [1, 2]. Piezoelectric MEMS devices typically consists of a membrane [3], a cantilever [4] or beam [5] with a piezoelectric layer deposited with sputtering [6], plasma-enhanced chemical vapor deposition (PECVD) [7], sol-gel spin-on [3, 15, 16] or screen printing [5, 8]. The piezoelectric ceramic $\text{Pb}(\text{Zr}_x\text{Ti}_{1-x})\text{O}_3$ (PZT) has a high coupling factor which makes it a interesting material for MEMS devices. The voltage sensitivity is for many MEMS devices proportional to the thickness of the piezoelectric film. Screen printing of PZT on Si substrates has shown promising results [8] and can be used to achieve thicker films compared to other deposition techniques [9, 10]. Integration of screen printed PZT thick film and MEMS technology introduces new challenges in the fabrication process as: alignment of the PZT film to the underlying MEMS structures, fine patterning of electrodes on the PZT thick film and a diffusion barrier layer between the PZT and the silicon substrate. All of these aspects are addressed in this work in order to form a MEMS based triaxial accelerometer.

MEMS based accelerometers are interesting as they have potential for being more cost efficient and miniaturized compared to conventional accelerometers [11]. MEMS based accelerometers can with advantage use the piezoelectric effect as their transducer element due to more controlled temperature dependence, no need for a stable driving source, better long term stability and higher possible bandwidth compared to the two other main transducer principles: capacitive and piezoresistive [12]. Applications for piezoelectric type

C. C. Hindrichsen (✉) · N. S. Almind ·
S. H. Brodersen · E. V. Thomsen
Department of Micro- and Nanotechnology,
Technical University of Denmark,
2800 Kgs. Lyngby, Denmark
e-mail: christian.hindrichsen@nanotech.dtu.dk

R. Lou-Møller
InSensor A/S, Kvistgaard, Denmark

K. Hansen
Ferroperm Piezoceramics A/S, Kvistgaard, Denmark

accelerometers would typically be for machine monitoring or automotive testing [13, 14]. These applications require high bandwidth with a maximal operation frequency of up to 15 kHz. For all accelerometer designs there will be a compromise between high sensitivity and high resonance frequency. Accelerometers with high resonance frequencies require thicker beams or membranes depending on the design. In order to have the neutral plane in the interface between the supporting material and the piezoelectric material for optimal sensitivity, thick piezoelectric films are required. Accelerometers with high resonance frequencies with screen printed PZT thick film therefore have a potential for higher voltage sensitivity compared to thin film based accelerometers.

2 Design and characterization

A single seismic mass triaxial accelerometer has theoretically no cross axis sensitivity and is therefore preferred compared to three single uniaxial accelerometers when monitoring a 3D acceleration. A triaxial accelerometer has a more complex design and requires comparable sensitivity for the three sensing directions in order to be able to distinguish the three components of the 3D acceleration vector.

Triaxial accelerometers typically have lower sensitivity compared to uniaxial accelerometers due to more limitations in their design. When comparing piezoelectric accelerometers three parameters are crucial: charge sensitivity, voltage sensitivity and the resonance frequency. A triaxial accelerometers with sol-gel deposited PZT have been reported in [15] with a sensitivity of 22 pC/g in the vertical direction and 8 pC/g in the horizontal direction. However no voltage sensitivity is presented and the resonance frequency is only 0.5 kHz making it unsuitable for high bandwidth applications. In [5] an accelerometer with screen printed PZT is presented with a charge sensitivity of 16 pC/g, a voltage sensitivity of 0.1 mV/g and a resonance frequency of 7.55 KHz but no triaxial detection has been reported. In [16] a sol-gel based two-dimensional accelerometer is presented with a charge sensitivity for the vertical direction of 0.12 pC/g and a voltage sensitivity of 0.1 mV/g and a resonance of 12.3 kHz but no sensitivity for the horizontal direction is presented.

In this paper we present how screen printed PZT thick film sandwiched between e-beam evaporated electrodes can be combined with a patterned silicon substrate to form a triaxial accelerometer with a high resonance frequency.

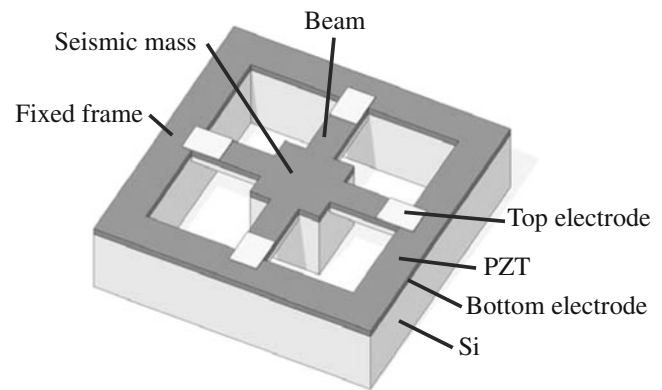


Fig. 1 The figure shows a conceptual drawing of the triaxial accelerometer

The accelerometer consists of a seismic mass suspended by four beams as shown in Fig. 1. The screen printing technique allows for thicknesses ranging 10–100 μm. The piezoelectric PZT is polarized orthogonal to the plane of the Si wafer. The bottom electrode covers the whole surface and the output signal is read out from the four individual top electrodes. The resonance frequency and the sensitivities are determined by the dimensions of the four supporting beams and the size of the seismic mass. The dimensions of the accelerometer are shown in Fig. 2 and Table 1.

2.1 Structure of triaxial accelerometer

The accelerometer has two modes of operation as shown in Fig. 3. For an acceleration in the vertical direction (z direction) all four beams, b_1 – b_4 , will have a symmetric deflection and four equal signals are read out from the four top electrodes. For an acceleration in the horizontal direction (x and y directions) the seismic mass will make a rotational movement and for a acceleration in the x direction the two beams b_1 and b_3

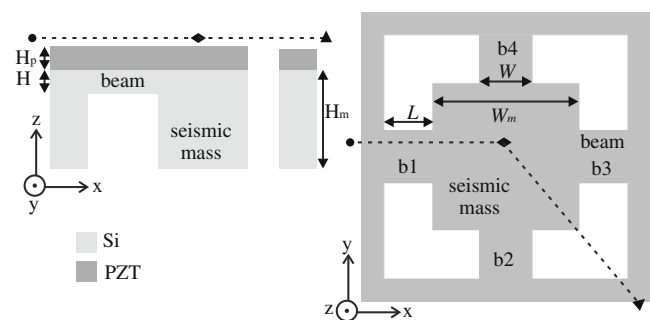


Fig. 2 Cross-sectional view (left) and top view (right) of the accelerometer including the six important dimensions

Table 1 The table shows the dimensions of the accelerometer and their abbreviation.

Thickness of the Si beam	H [μm]	20
Thickness of the PZT	H_p [μm]	30
Width of the beam	W [μm]	600
Length of the beam	L [μm]	800
Thickness of the seismic mass	H_m [μm]	520
Width of the seismic mass	W_m [μm]	1200
Active area of the top electrode	A_1 [mm^2]	0.24
Passive area of the top electrode	A_2 [mm^2]	0.24
Die size	[mm]	10×10

along the direction of the acceleration will have an anti-symmetric deflections. The two beams b_2 and b_4 orthogonal to the direction of the acceleration will rotate along their length axis and due to symmetry no signal will be read out from the top electrodes on the beams b_2 and b_4 . Due to symmetry the same will be the case for acceleration in the y direction. Using additional signal processing the three signals can be distinguished from each other. However, reading out the three individual signals is only possible if the sensitivity for the three directions are similar. A optimal accelerometer design should also have the same resonance frequencies for the vertical movement as for the horizontal movement.

2.2 Electrical properties of triaxial accelerometer

Based on the equations presented in this section and a FEM model the theoretical sensitivities and resonance frequency are found. The mechanical movement of the seismic mass due to an acceleration induces a stress, $[\sigma]$, in the PZT layer. The piezoelectric effect in the stressed PZT layer results in an electric field, $[E]$, between the top and bottom electrode [17],

$$[E] = -[g][\sigma], \tag{1}$$

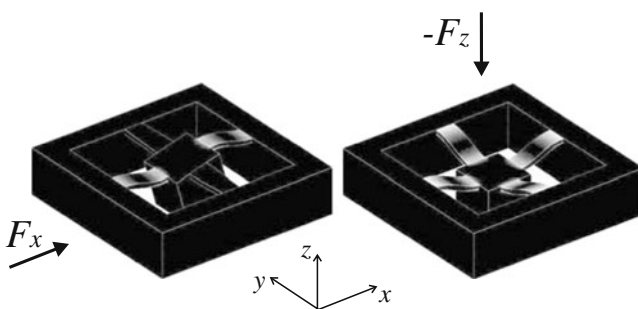


Fig. 3 The figure shows the two modes of operation, a horizontal acceleration (left) and a vertical acceleration (right). The color indicates the strain energy density, $[\text{Jm}^{-3}]$, in arbitrary units where the bright color represents a large value

where six vector notation is used and $[g]$ is the piezoelectric voltage coefficient given as,

$$[g] = \begin{bmatrix} 0 & 0 & 0 & 0 & g_{15} & 0 \\ 0 & 0 & 0 & g_{24} & 0 & 0 \\ g_{31} & g_{32} & g_{33} & 0 & 0 & 0 \end{bmatrix}. \tag{2}$$

The voltage sensitivity, S_V , with the unit Vs^2/m is the potential difference between the top and bottom electrode per acceleration [18],

$$S_V = \bar{E}_3 \frac{A_2}{A_1 + A_2} H_p \tag{3}$$

where \bar{E}_3 is the mean electric field in the active PZT between the top and bottom electrode in the z direction. H_p is the distance between the top and bottom electrode as well as the thickness of the PZT layer. A_1 and A_2 are the xy areas of the non stressed and stressed PZT respectively as shown in Fig. 4. Only in the stressed PZT, also called the active PZT, charge will be generated. The mean electric field is different for the two modes of operation which results in different sensitivities for the vertical and horizontal acceleration. The wires and bonding pads for the top electrode which contribute to the area A_1 should be minimized as much as possible in order to have a high voltage sensitivity. The electric field is found using a 3D FEM model made in Comsol Multiphysics 3.3.

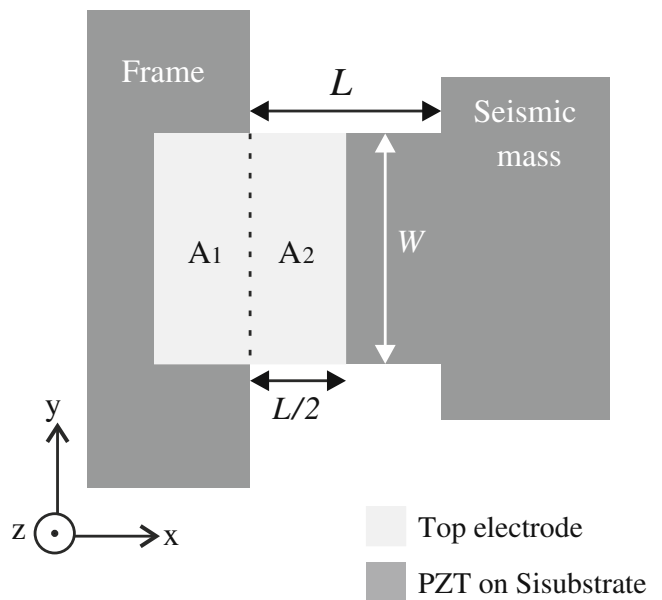


Fig. 4 A top view of one of the four beams connecting the seismic mass to the frame is seen

Table 2 The table shows the important material parameters used in the FEM model.

Material	PZT	Si
$Y [10^9 \text{ Pa}^{-1}]$	142.5	70.2
Density, $\rho [\text{kgm}^{-3}]$	6740	2330
$g_{31} [10^{-3} \text{ VmN}^{-1}]$	-9	-
$g_{33} [10^{-3} \text{ VmN}^{-1}]$	39	-
ϵ_r	640	-

Parameters related to the PZT thick film are supplied by InSensor A/S

The capacitance of each of the four active PZT areas based on a simple plate capacitor model is given by,

$$C_{PZT} = \frac{A_1 + A_2}{H_p} \epsilon_r \epsilon_0 \tag{4}$$

where ϵ_r is the relative permittivity and ϵ_0 is the vacuum permittivity ($8.85 \times 10^{-12} \text{ F/m}$). The charge sensitivity, S_Q , measured in Cs^2/m defines the amount of short circuited charge generated on the electrodes by the active PZT per acceleration and is a function of the capacitance and the voltage sensitivity,

$$S_Q = C_{PZT} S_V = A_2 \bar{E}_3 \epsilon_r \epsilon_0 \tag{5}$$

High charge sensitivity reduces the effect of parasitic capacitances and improves the signal to noise ratio.

In order to optimize the sensitivity a maximum amount of energy should be used for stressing the PZT layer meaning the neutral plane of the deflected beam optimally should be situated in the interface between the silicon beam and the PZT layer. This is ensured by setting the ratio between the thicknesses of the silicon beam and the PZT film as [19],

$$H_p = H \sqrt{\frac{Y_{Si}}{Y_{PZT}}} \tag{6}$$

assuming that the widths of the layers are equal which is the case for this accelerometer design. Y_{Si} and Y_{PZT} are the Young’s modulus for silicon and PZT respectively. The mechanical influence of the top and bottom electrode is neglected due to their small thicknesses. Table 2 shows the material parameters used in the FEM model.

3 Experiments

A schematic drawing of the fabrication process flow is shown in Fig. 5. A 500 μm thick double-side polished (100) 4” Silicon On Insulator (SOI) wafer with a 20 μm device layer is used as substrate material. Three

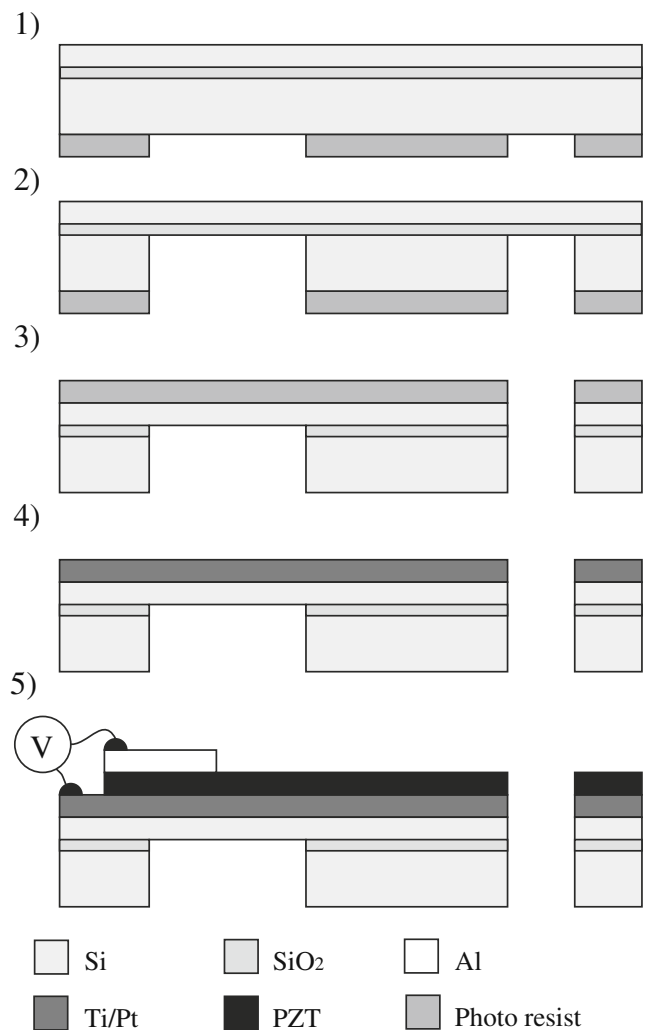


Fig. 5 The figure shows a cross sectional view (see Fig. 2) of the process flow starting out with a SOI wafer

photolithographic masks and an additional mask for the screen printing process are used in the fabrication process.

3.1 MEMS process flow

An Advanced Silicon Etch (ASE) process is used for thinning down the beams from the backside to get the desired beam thicknesses, H (steps 1 and 2), defined by the device layer. For releasing the seismic mass and the beams a second ASE process is used from the front side (step 3). A handle wafer is bonded to the backside enabling a through-etch of the wafer. Standard positive photoresist (AZ4562) with a thickness of 9.5 μm is used as masking material for both ASE processes. A dedicated diffusion barrier layer also working as bottom

electrode is e-beam deposited on the front side on a grown SiO_2 layer (step 4). The combination $\text{SiO}_2/\text{Ti}/\text{Pt}$ with the thicknesses 500/50/500 nm has proven to be a good diffusion barrier layer between the Si substrate and the PZT thick film at the high sintering temperatures [20].

3.2 PZT thick film process by screen printing

Following the conventional MEMS processing a 30 μm thick PZT paste (InSensor TF2100) is screen printed through a 77T polyester mesh mask on the front side (step 5). The screen printing process is schematically illustrated in Fig. 6. Screen printing has a resolution down to around 100 μm which is not enough to pattern the PZT elements accurately on the beams. The screen printing mask therefore only defines the coarse pattern of the PZT thick film. The PZT paste is screen printed over the holes defining the seismic mass and the four beams. At the places where the substrate material has been etched away the paste will keep sticking to the fine mesh and thereby be removed again as the screen printing mask mesh is removed. In this way the screen printed thick film is patterned with the resolution of the ASE process. This has not been done before and the results presented here are the initial attempts using whole in the substrate for fine patterning of the PZT thick film. After screen printing the PZT is sintered for one hour at 850°C [8]. It proved possible to successfully screen print on silicon beams with thicknesses down to 20 μm without breaking them.

A 500 nm Al top electrode is e-beam deposited on the PZT (step 5) and the PZT thick film is finally poled at 150°C with a field of around 10 kV/mm for 10 min in order to obtain the piezoelectric properties of the PZT layer.

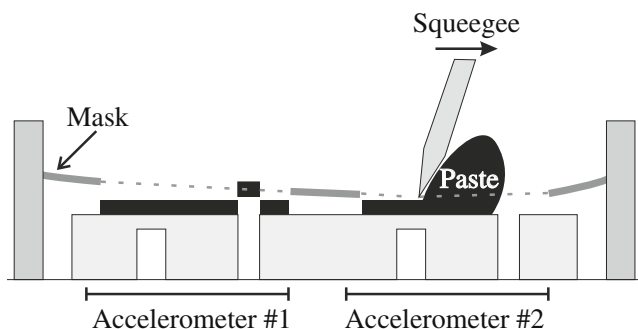


Fig. 6 Schematic drawing of the screen printing process of two adjacent accelerometers

4 Results and discussion

Figure 7 shows the accelerometer from the top with the seismic mass suspended by the four beams. The PZT thick film is not completely well defined as part of the PZT thick film is going over the edges of the patterned Si substrate. In the worst case the overhanging of the PZT has a width of 200 μm , which influences the mechanical behavior significantly. The extra PZT influences the stress distribution in the active PZT elements and thereby lower the sensitivity significantly. The resonance frequency is also slightly affected due to a more damped structure. This extra unwanted PZT is difficult to include in the FEM model due to its randomness and the FEM model therefore only is done for a perfect well defined structure. The technique with using the holes in the substrate for masking of the PZT layer needs further improvements, as the yield currently is around only 20%. However the initial investigations show promising results.

The PZT thick film has grain sizes of around 1 μm and as Figs. 8 and 9 shows there is a good grain size distribution. The SEM image in Fig. 8 shows the interface between the silicon substrate and the porous PZT thick film. The thin diffusion barrier layer consisting of $\text{SiO}_2/\text{Ti}/\text{Pt}$ clearly prevents diffusion of silicon or silicon oxide into the PZT which also verified with EDX measurements. The thicknesses of the metal layers are verified before sintering. Figure 8 indicates that the metal layers appear rougher after the sintering process. However, their purposes as conducting bottom electrode and diffusion barrier layers are unaffected.

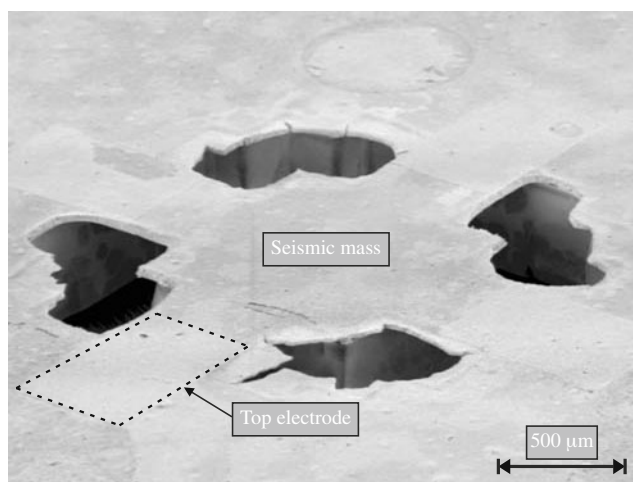


Fig. 7 The SEM image shows the seismic mass suspended by the four beams seen from the front side with the PZT thick film and four top electrodes

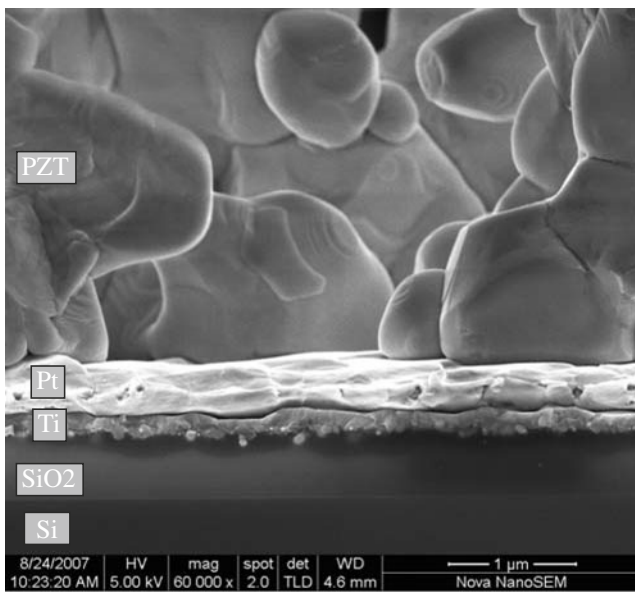


Fig. 8 The cross-sectional SEM image shows the Si-PZT interface with the diffusion barrier layer in-between

Figure 9 shows the PZT thick film on the 20 μm thick Si beam and the PZT layer thickness is very well defined and is measured to be 30.9 μm. The microstructure of the film has been investigated in previous work [8].

4.1 Shaker setup

In order to find the resonance frequency and the sensitivity the accelerometer is mounted onto a shaker (B&K Mini Shaker 4810), together with a reference accelerometer (B&K Piezoelectric Accelerometer 8305).

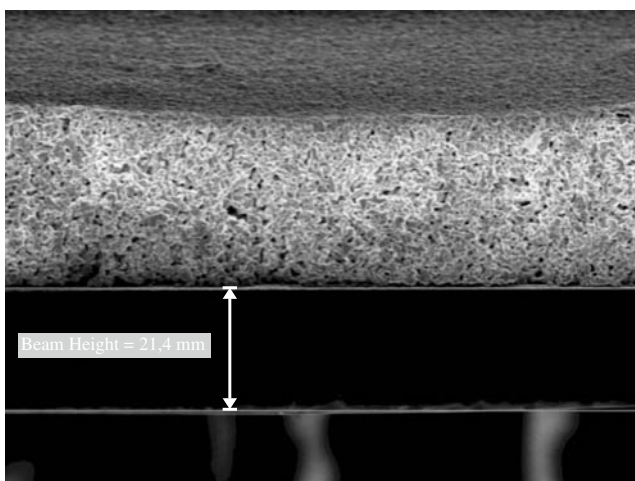


Fig. 9 A 30.9 μm thick PZT layer seen from the side has been screen printed onto the 20 μm thick Si beam

The shaker is driven by a wave generator (Agilent 33220A) through an amplifier. The output signal from the PZT accelerometer and the reference accelerometer are amplified with a charge amplifier converting the high impedance signal from the PZT into a measurable low impedance signal. The RMS value of the output signal is read out with an oscilloscope (HP 54522A). The charge sensitivity, S_Q , is given as [21],

$$S_Q = \frac{V_{out}}{V_{out}^{ref}} S_Q^{ref} \tag{7}$$

where S_Q^{ref} is the charge sensitivity for the reference accelerometer and V_{out} and V_{out}^{ref} are the RMS values of the voltage signal read out with the oscilloscope. The accelerometer chip is glued onto a printed circuit board which is screwed onto an aluminum sample holder. The sample holder is screwed on top of the reference accelerometer. The sample holder is turned 90 degrees with sub-degree precision in an upright position for characterization of the horizontal direction.

4.2 Sensitivity

The sensitivity is measured for changing accelerations at a fixed frequency of 2 kHz. Figure 10 shows the charge generated in the PZT for the accelerometer positioned in the flat and in the upright position for accelerations ranging from about 0.5 g up to 6 g which is the upper limit of the setup. The slope of the two fitted lines equal the sensitivities for the vertical and horizontal direction respectively. Good linearity for

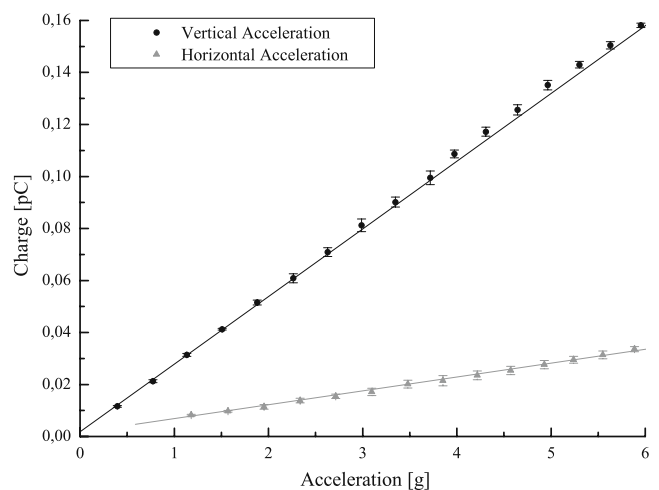


Fig. 10 The charge generated in the PZT is plotted as a function of acceleration at constant frequency (2 kHz). The vertical sensitivity is measured by positioning the accelerometer in the flat position and the horizontal is measured by positioning the accelerometer in an upright position

the two directions is seen and the linear fits show a very small offset. The measured charge sensitivities are 0.0260 pC/g and 0.0053 pC/g for the vertical and horizontal direction respectively. The capacitance for a single electrode is measured to be 86 pF and with Eq. 5 the voltage sensitivities are found to be 0.31 mV/g and 0.062 mV/g for the vertical and horizontal direction respectively.

4.3 Resonance frequency

By feeding the shaker with a white noise signal and performing a Fast Fourier Transformation (FFT) of the output signal the resonance frequencies at high frequencies can be studied. Figure 11 shows the FFT spectra for the accelerometer when positioned in the flat and in the upright position respectively. In the flat position the dominant peak is observed at around 11 kHz. In the upright position a peak at around 23 kHz is seen which is close to the modeled resonance frequency for the horizontal direction.

4.4 Discussion

Table 3 summarizes the measured sensitivities and resonance frequencies as well as the measured capacitances and compares them with the values found with the FEM model. The charge sensitivity is measured directly whereas the voltage sensitivity is a function of the charge sensitivity and the capacitance. Both the sensitivity in the vertical and in the horizontal direction are

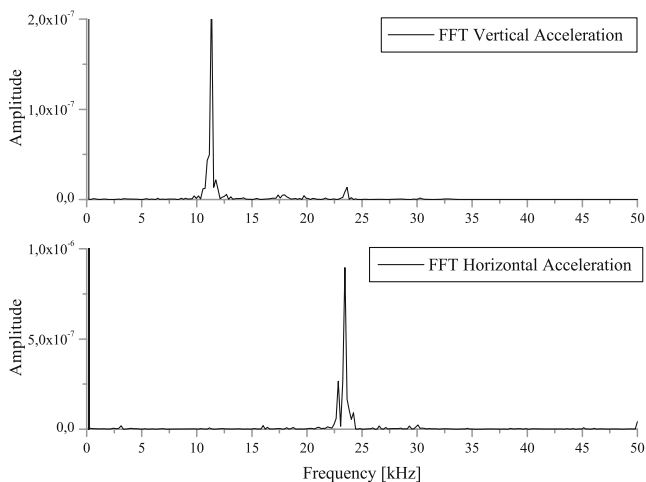


Fig. 11 The figure shows two FFT plots from the accelerometer when the shaker is feeded with a white noise signal. In the *upper plot* the accelerometer is positioned in a flat position and the accelerometer experience a vertical acceleration. In the *lower plot* the accelerometer is positioned in an upright position and the accelerometer experience a horizontal acceleration

Table 3 The table shows the measured and modeled sensitivities and resonance frequencies of the accelerometer.

	FEM	Measured
C [pF]	–	86
Vertical		
S_V [mV/g]	0.36	0.31
S_Q [pC/g]	0.038	0.0260
f_v [kHz]	12.5	11
Horizontal		
S_V [mV/g]	0.10	0.062
S_Q [pC/g]	0.011	0.0053
f_h [kHz]	25.5	23

about half the values found with the the FEM model. This can partly be explained by the not completely well defined PZT thick film as shown in Fig. 7 which increases the stiffness of the beams. Good agreement is found when comparing the resonance frequencies both in the vertical and in the horizontal direction. However, the completely well defined PZT thick film would also result in higher resonance frequencies compared to the model, which is not observed.

Therefore other reasons such as lower piezo coefficients than expected could be an explanation for the measured lower sensitivity. This explanation is supported by the lower measured capacitance. Experience show that lower the piezo coefficients also result in a lower the permittivity. The geometries of the top electrodes are very well defined and the lower capacitance is therefore due to a lower permittivity.

However, it is believed that the main reasons for the deviation between the measured and modeled sensitivity is a change in the stress distribution due to the bridging show in Fig. 7. The extra PZT will not affect the stiffness of the beam significantly as the resonance frequency measurements also indicate. If the distribution of the stress is changed, resulting in a lower mean stress in the active PZT, the sensitivity will be decreased as the amount of generated charge decreased.

All though the resonance frequency in the horizontal direction is found to be 23 kHz the operational bandwidth is defined by the first resonance frequencies at 11 kHz. In an improved accelerometer design the resonance frequency for the vertical and horizontal direction should be closer to each other. The sensitivities would thereby also be comparable in size. A way to get close sensitivity among the three directions would be to have a thicker seismic mass which would increase the horizontal sensitivity relatively more than the vertical.

In Wang et al. [10] a piezoelectric accelerometer with a charge sensitivity of 1.45 pC/g and a resonance frequency of 17.4 has been reported. This is several

order of magnitude larger compared to the thick film based accelerometer reported here. However, the main advantage of thick film based accelerometer compared to thin film based accelerometers is a higher voltage sensitivity which is not reported in [10]. Nevertheless the charge sensitivity must be increased in future designs by mainly improving the properties of the PZT thick film. A more dense PZT film would increase the piezoelectric voltage coefficient, lower the porosity and thereby increase the Young's modulus of the PZT film, which all would contribute to a higher charge sensitivity and voltage sensitivity.

5 Conclusion

In conclusion, MEMS and thick film screen printing technology have successfully been combined to fabricate a low cost accelerometer with a simple fabrication process only using three lithographic masks and one for the screen printing process. The voltage sensitivity at 2 kHz is measured to be 0.31 mV/g and 0.062 mV/g for the vertical and horizontal direction respectively. The first resonance peak is found to be at 11 kHz and the second at 23 kHz which is in good agreement with the modeled frequencies.

The results show that the presented accelerometer is a good candidate for applications requiring a high bandwidth. With an improved design of the accelerometer and minor improvements of the fabrication process higher sensitivities and higher resonance frequencies are possible. The PZT thick film should be better defined in future designs else it will be a too significant source of error. Further characterization should be performed especially regarding cross axis sensitivity which is very important for triaxial accelerometers.

Acknowledgements This research is a collaboration between “The Department of Micro and Nanotechnology” (DTU Nanotech) and the two companies InSensor A/S and Ferroperm Piezoceramics A/S. It is part of the PiMEMS project which is supported by “The Danish National Advanced Technology Foundation”.

References

1. S. Trolier-McKinstry, P. Muralt, Thin film piezoelectrics for MEMS. *Journal of Electroceramics* **12**(1–2), 7–17 (2004)
2. R.A. Dorey, R.W. Whatmore, Electroceramic thick film fabrication for MEMS. *Journal of Electroceramics* **12**, 19–32 (2004)
3. P. Muralt, N. Ledermann, J. Baborowski, A. Barzegar, S. Gentil, B. Belgacem, S. Petitgrand, A. Bosseboeuf, N. Setter, Piezoelectric micromachined ultrasonic transducers based on PZT thin films. *IEEE Trans. Ultrason. Ferroelectr. Freq. Control* **52**(12), 2276–2288 (2005)
4. J.H. Park, T.Y. Kwon, D.S. Yoon, T.S. Kim, Effect of the porosity of PZT thick films on mass sensitivity and resonance force for cantilever type biosensors, in *6th IEEE Sensors Proceeding*, (2006), pp. 1219–1222
5. S.P. Beeby, J.N. Ross, N.M. White, Design and fabrication of a micromechanical silicon accelerometer with thick-film printed PZT. *J. Micromechanics Microengineering* **10**, 322–328 (2000)
6. H. Jacobsen, H.J. Quenzer, B. Wagner, K. Ortner, Th. Jung, Thick PZT layers deposited by gas flow sputtering. *Sens. Actuators, A* **135**(1), 23–27 (2007)
7. Q. Zou, W. Tan, E.S. Kim, G.E. Loeb, Single- and triaxis piezoelectric-bimorph accelerometers. *Journal of Microelectromechanical Systems* **17**(1), 45–57 (2008)
8. R. Lou-Møller, C.C. Hindrichsen, L.H. Thamdrup, T. Bove, E. Ringgaard, A.F. Pedersen, E.V. Thomsen, Screen-printed piezoceramic thick films for miniaturised devices. *Journal of Electroceramics* **19**(4), 333–338 (2007)
9. F.F.C. Duval, R.A. Dorey, R.W. Wright, Z. Huang, R.W. Whatmore, Fabrication and modeling of high-frequency PZT composite thick film membrane resonators. *IEEE Trans. Ultrason. Ferroelectr. Freq. Control* **51**(10), 1255–1261 (2004)
10. L. Wang, R.A. Wolf Jr., Y. Wang, K.K. Deng, L. Zou, R.J. Davis, S. Trolier-McKinstry, Design, fabrication, and measurement of high-sensitivity piezoelectric microelectromechanical systems accelerometers. *Journal of MEMS* **12**(4), 433–439 (2003)
11. P. Scheeper, J.O. Gulløv, L.M. Kofoed, A piezoelectric triaxial accelerometer. *J. Micromechanics Microengineering* **6**, 131–133 (1996)
12. G.H. Gauschi, *Piezoelectric Sensorics* (Springer, 2002)
13. J.C. Robinson, J.M. Rybak, E.R. Saller, Using accelerometers to monitor complex machinery vibration. *Sensors* **14**(6), 36–42 (1997)
14. D. Lyon, Good vibrations, *Electron. World* **113**(1857), 36–38 (2007)
15. K. Kunz, P. Enoksson, G. Stemme, Highly sensitive triaxial silicon accelerometer with integrated PZT thin film detectors. *Sens. Actuators, A* **92**, 156–160 (2001)
16. D. Eichner, M. Giousouf, W. von Munch, Measurements on micromachined silicon accelerometers with piezoelectric sensor action. *Sens. Actuators, A* **76**, 247–252 (1999)
17. B. Jaffe, W.R. Cook, H. Jaffe, *Piezoelectric Ceramics* (Academic Press, London New York, 1971)
18. C.C. Hindrichsen, N.S. Almind, S.H. Brodersen, O. Hansen, E.V. Thomsen, Analytical model of a PZT thick-film triaxial accelerometer for optimum design. *IEEE Sens. J.* **9**(4), 419–429 (2009)
19. S.P. Timoshenko, J.N. Goodier, *Theory of Elasticity* (McGraw-Hill Education, 1970)
20. T. Pedersen, C.C. Hindrichsen, R. Lou-Møller, K. Hansen, E.V. Thomsen, Investigation of top/bottom electrode and diffusion barrier layer for PZT thick film MEMS sensors, in *6th IEEE Sensors Proceeding*, (2007), pp. 756–759
21. S.H. Choy, X.X. Wang, H.L.W. Chan, C.L. Choy, Study of compressive type accelerometer based on lead-free BNKBT piezoceramics. *Appl. Phys.*, **A** **82**, 715–718 (2006)